Study of Radial Particle Transport Accompanied with Plasma Blob and Self-organized Meso-scale Structure in Tokamak Scrape-off Layer

S. Sugita 1), M. Yagi 2, 3), S.-I. Itoh 2), K. Itoh 4)

1) Interdisciplinary Graduate School of Engineering Sciences (IGSES), Kyushu University, Kasuga, Japan
2) Research Institute for Applied Mechanics (RIAM), Kyushu University, Kasuga, Japan
3) Japan Atomic Energy Agency (JAEA), Naka, Japan
4) National Institute for Fusion Science (NIFS), Toki, Japan

E-mail contact of main author: satoru@riam.kyushu-u.ac.jp

Abstract. The non-diffusive radial transport in the SoL is investigated using the 2D SoL interchange turbulence simulation code, which reproduces plasma blobs. From the nonlinear simulations, it is found that the meso scale convective cells emerge from interchange instabilities and propagate in the radial direction. The structures are formed by the inverse cascade of the convective turbulence autonomously. The radial propagation velocity of the blob structure and the effective SoL radial convective transport velocity are compared with each other. It is found that both quantities agree fairly well. The effective transport coefficient is also evaluated and the Bohm-like dependence is found. It is concluded that the flux-driven turbulence in SoL, induces Bohm-like 'non-diffusive' transport.

1. Introduction

Recently, the importance of blobs formation in the process of cross-magnetic-field-transport in the SoL has attracted attention. The blobs are high-density magnetic-field-aligned filaments, and have been observed in several experimental devices [1-3]. The 'non-diffusive' transport accompanied by blobs flattens the density profile in SoL and is attributed to the increase of impurities and the recycling rate at the first wall [4]. The concept of a plasma blob was discussed in literature [5]. Dynamics during radial propagation of a single blob in the SoL are studied based on this model [6,7]. It is an urgent task to understand the formation process of blobs in the edge turbulence and to have an insight into the associated global transport. This article discusses the 'non-diffusive' transport in SoL by the simulation of flux-driven turbulence.

2. Model and Simulation Setup

The two-dimensional Hasegawa-Wakatani-type model equation is introduced, which describes plasma blob behavior in the SoL as well as SoL interchange turbulence [8]. In this model, the SoL plasma is assumed to be a magnetic-field aligned flux tube, and both ends of each field line terminate at grounded conducting plates. Taking the sheath boundary conditions into account, the vorticity equation and continuity equation can be reduced to a two-dimensional slab geometry by integrating along the magnetic field lines, where all quantities except the current are assumed to be constant along **B**.

$$\frac{\partial}{\partial t}\nabla_\perp^2\varphi + \left[\varphi, \nabla_\perp^2\varphi\right] = \alpha\varphi - \frac{\beta}{n}\frac{\partial n}{\partial y} + \mu\nabla_\perp^4\varphi, \tag{1}$$

$$\frac{\partial n}{\partial t} + [\varphi, n] = -\alpha n + \beta\left(n\frac{\partial\varphi}{\partial y} - \frac{\partial n}{\partial y}\right) + D\nabla_\perp^2 n + S\,(x)\,, \tag{2}$$

where x is the radial direction and y is the poloidal direction, $[f, g] = (\partial f / \partial x)(\partial g / \partial y) - (\partial f / \partial y)(\partial g / \partial x)$ is the Poisson bracket, n is the plasma density, φ is the electrostatic potential, μ is

the ion viscosity and D is the collisional diffusion coefficient. The characteristic parameter $\alpha = 2\rho_s / L_{\parallel}$ is a measure of the net parallel current into the divertor plates, and $\beta = 2\rho_s / R$ is a measure of the strength of the curvature drift. $\rho_s = c_s / \Omega_i$ is the ion Larmor radius, c_s is the ion acoustic speed, and Ω_i is the ion cyclotron frequency. R is the tokamak major radius, $L_{\parallel} = qR$ is the connection length of the magnetic field line in the SoL, and q is the safety factor. The other parameters have their usual meanings. The length and time are normalized to ρ_s and Ω_i^{-1}, respectively. $S(x)$ is the plasma source, which is supplied from core to SoL, and is given by a Gaussian shape such as $S(x) = S_0 \exp(-x^2 / \lambda^2)$, where $S_0 = 5 \times 10^{-3}$ and $\lambda = 8$. The source is introduced at the $x = 0$ boundary in the numerical simulation.

The model equations are solved numerically by the finite difference method in the x direction and by a Fourier expansion in the y direction. The following boundary conditions are imposed in the x direction. In the vorticity equation,

$$
\begin{aligned}
&m = 0 \text{ mode:} && \varphi'(x = 0) = 0, && \varphi(x = L_x) = 0,\\
& && \nabla_\perp^2 \varphi'(x = 0) = 0, && \nabla_\perp^2 \varphi(x = L_x) = 0,\\
&m \neq 0 \text{ mode:} && \varphi(x = 0) = 0, && \varphi(x = L_x) = 0,\\
& && \nabla_\perp^2 \varphi(x = 0) = 0, && \nabla_\perp^2 \varphi(x = L_x) = 0.
\end{aligned}
$$

Here, the prime indicates the derivative with respect to x and L_x indicates the system size in the x direction. Likewise, in the continuity equation, the conditions,

$$
\begin{aligned}
&m = 0 \text{ mode:} && n'(x = 0) = 0, && n(x = L_x) = 0,\\
&m \neq 0 \text{ mode:} && n(x = 0) = 0, && n(x = L_x) = 0
\end{aligned}
$$

are imposed. A periodic boundary condition is used in the y direction such that $\varphi(y = 0) = \varphi(y = L_y)$ and $n(y = 0) = n(y = L_y)$, where L_y indicates the system size in the y direction. The simulation box size is set up as $L_x = L_y = 256$ (in units of ρ_s). For dissipation parameters, $\mu = D = 2 \times 10^{-2}$ are assumed. For the characteristic parameters α and β, $\alpha = 3 \times 10^{-5}$ and $\beta = 6 \times 10^{-4}$ are used for the reference case. These values are obtained by assuming $c_s = 6 \times 10^4$ [m / sec], $\Omega_i = 10^8$ [sec^{-1}], $L_{\parallel} = 40$ [m], and $R = 2$ [m] [7]. (Dependence on the system size has been discussed in [8], and we have confirmed that the system size does not limit the transport phenomena.)

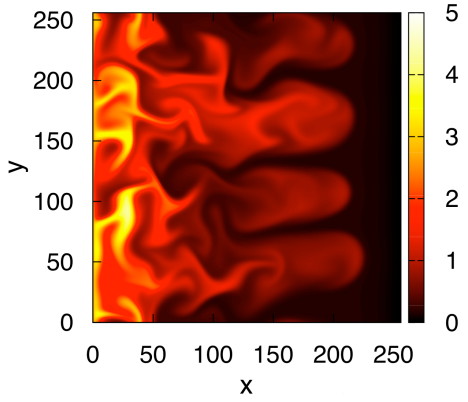

FIG. 1. Snapshot (t = 5500) of density contour. Unit of length is ion Larmor radius.

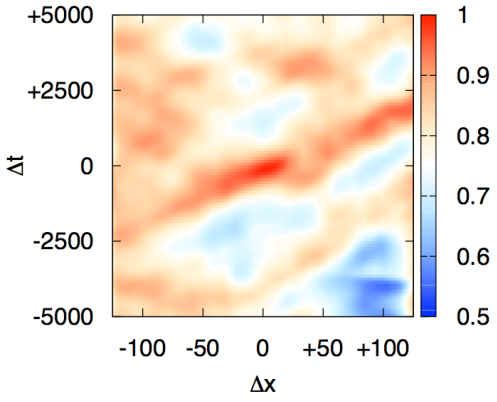

FIG. 2. Space-time correlation of turbulence-driven flux which is averaged in y-direction.

3. Radial Transport and the velocity

The non-diffusive radial transport in the SoL is investigated using the 2D SoL turbulence simulation code, which reproduces plasma blobs. The curvature (represented by β) drives SoL interchange instability, and larger α is effective for the stabilization. From the nonlinear simulations, it is shown that the meso-scale convective cells emerge from interchange instabilities and propagate in the radial direction (see FIG.1.). The meso-scale structures are formed by the inverse cascade of the convective turbulence autonomously. The poloidally averaged turbulence-driven (Γ_t) and diffusive (Γ_d) particle fluxes are evaluated as following:

$$\Gamma_t(x) = \frac{1}{L_y}\int_0^{L_y} \tilde{n}(x,y)\left(-\nabla_y \tilde{\varphi}(x,y)\right)\,\mathrm{d}y, \tag{3}$$

$$\Gamma_d(x) = -D\frac{\partial}{\partial x}\frac{1}{L_y}\int_0^{L_y} n(x,y)\,\mathrm{d}y. \tag{4}$$

The phase relation between the turbulence-driven flux at two different radial positions allows us to estimate the spatiotemporal characteristics of the SoL radial turbulent transport. The auto-correlation function is defined by

$$C(\Delta x, \Delta t) = \frac{\langle \Gamma_t(x_0+\Delta x, t_0+\Delta t)\,\Gamma_t(x_0,t_0)\rangle}{\sqrt{\left\langle \Gamma_t^2(x_0+\Delta x, t_0+\Delta t)\right\rangle \left\langle \Gamma_t^2(x_0,t_0)\right\rangle}}, \tag{5}$$

where (x_0, t_0) indicates the reference position for the auto-correlation function; $x_0 = 128$ and $t_0 = 10000$ are used. $< >$ indicates the temporal average defined as $\langle f(t)\rangle = T^{-1}\int_t^{t+T} f(s)\,\mathrm{d}s$ with $T = 10000$. The auto-correlation averaged in the y-direction (poloidal direction) is measured. The auto-correlation is elongated from the separatrix to the first wall as is clearly demonstrated in FIG.2. This indicates that the SoL radial transport is strongly ballistic. It is considered that the convective transport accompanied with the meso-scale self-organized structures dominate the radial transport in the SoL. In this simulation, the size of the blob structure is self-organized as a consequence of the evolution of the instabilities. The selection rule for the size of blobs and radial velocity of blobs are understood as follows. The scale length is determined by the balance between two mechanisms that deform the blob. Small blobs break up via the Kelvin-Helmholtz (K-H) instability. They spread and gather to form larger structures. Large blobs break up with the interchange instability [7]. The balance between these two competing processes determines the characteristic scale length, which is in proportion to $\beta^{1/5}\alpha^{-2/5}$. Using this size in the y-direction, the radial propagation velocity of the blob structure is given as following:

$$V_x \sim 0.5\beta^{3/5}\alpha^{-1/5}\left[\sim 0.66\,(L_\parallel/R)^{1/5}\,(\rho_s/R)^{2/5}\,c_s \text{ in dimensional unit}\right]. \tag{6}$$

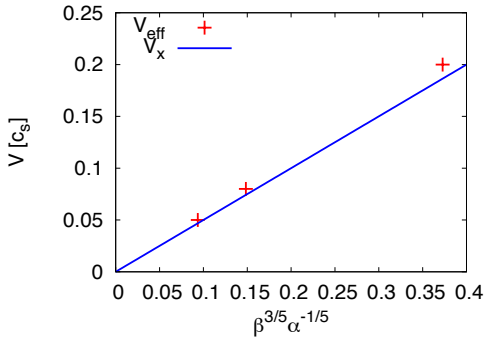

FIG. 3. Comparison between V_x and V_{eff} estimated from nonlinear simulation. Unit of velocity [c_s] indicates ion sound

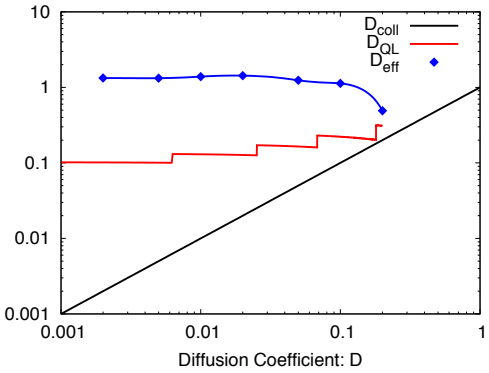

FIG. 4. D dependence of collisional diffusion coefficienrt D_{coll}, quasi-linear estimation of turbulent diffusion coefficient D_{QL}, and effective diffusion coefficient D_{eff} obtained by nonlinear simulation.

The velocity V_x is compared to the SoL radial convective transport velocity estimated from the slope of the spatiotemporal correlation ($V_{\rm eff}$) and they agree well each other (see FIG.3.) [5]. The nonlinear simulation is performed for the following three cases. (Ref. case) $\alpha = 3 \times 10^{-5}$, $\beta = 6 \times 10^{-4}$, (Low α case) $\alpha = 3 \times 10^{-6}$, $\beta = 6 \times 10^{-4}$, (High β case) $\alpha = 3 \times 10^{-5}$, $\beta = 6 \times 10^{-3}$. $V_{\rm eff}$ points in FIG.3. are Ref., Low α, and High β from the left. We have investigated the effect of the parameter D, i.e., the collisional diffusion coefficient, on the turbulent transport associated with the meso-scale structures. We have confirmed that the SoL turbulent transport via blob formation is weakly dependent on D, except when D is exceptionally large. It would be advantageous that determine the order of magnitude of D by comparing it with the quasi-linear estimation obtained by Kadomtsev [9], $D_{\rm QL} \sim \gamma_{\rm L}/k_y^2$, where $\gamma_{\rm L}$ is the maximum linear growth rate (for the interchange instability occurring in the region of the source) and k_y is the wave number of the most unstable mode. FIG.4. shows the effect of the parameter D on the effective transport coefficient for blob transport, $D_{\rm eff}$, and a comparison of $D_{\rm QL}$ with D. (The wave numbers are discrete because the system size is finite, thus, $D_{\rm QL}$ is discretized here.) We introduce the effective transport coefficient $D_{\rm eff}$ in nonlinear simulations using the ratio of the turbulence-driven flux $\Gamma_{\rm t}$ to the collisional diffusive flux $\Gamma_{\rm d}$ as

$$D_{\rm eff} = (\Gamma_{\rm t}/\Gamma_{\rm d})\, D. \tag{7}$$

The nonlinear simulation is demonstrated for some cases from $D = 2 \times 10^{-3}$ to 2×10^{-1}. The time average is taken from $t = 10000$ to 30000 to study the quasi-steady state. In the space, $\Gamma_{\rm t}$ and $\Gamma_{\rm d}$ are averaged over the y-direction and $L_x/4$ to $3L_x/4$ in the x-direction to calculate $D_{\rm eff}$. In FIG.4., we plot D as $D_{\rm coll}$, $D_{\rm QL}$, and $D_{\rm eff}$. We see that the value of $D \sim 0.1$ is impractically large as it is on the order of the Bohm diffusion coefficient. Upon choosing a realistic value for the collisional diffusion coefficient ($D < 0.1$), the turbulence-driven flux dominates the transport. Moreover, for small values of D, in which meso-scale fluctuations develop, the result is independent of D. The default parameter for D is assumed to be $D = 2 \times 10^{-2}$. Compared with those for the smallest value of D ($D = 2 \times 10^{-3}$), the characteristic size of the meso-scale structure is not different, the peak position of the k_y spectra is not affected, and the k_y spectra show the same tendency. Thus, the result for the reference case is considered to be almost independent of the choice of the parameter D.

We next study the dependence of effective diffusivity $D_{\rm eff}$. We performed parameter survey for several α and β (see FIGs.5. and 6.). In the small $D_{\rm eff}$ region ($D_{\rm eff} < 2$), where the effective diffusion coefficient is much larger than the quasi-linear estimate $\gamma_{\rm L}/k_y^2$, We have the following Bohm-like dependence:

$$D_{\rm eff} \propto (\beta/\alpha)^{2/5} \ [\sim (L/R)^{2/5}\, \rho_{\rm s} c_{\rm s} \text{ in dimensional unit}]. \tag{8}$$

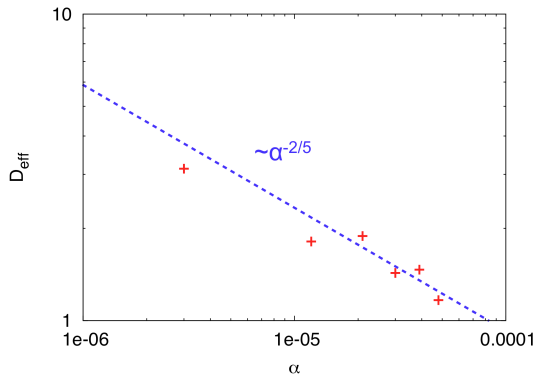

FIG. 5. Parallel current parameter α dependence of effective diffusion coefficient D_{eff}.

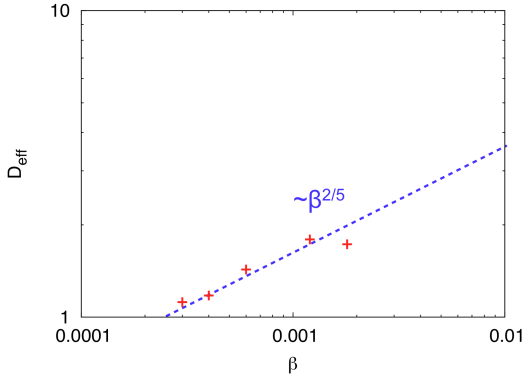

FIG. 6. Curvature parameter β dependence of effective diffusion coefficient D_{eff}.

This estimation equation is given by a inductive approach such that the fitting of data of nonlinear simulations. Reviewing the eqs.(6) and (8), we get the following relation:

$$D_{\text{eff}} \propto (\alpha\beta)^{-1/5} V_x. \tag{9}$$

Assuming that the effective transport in the SoL is dominated by the blob transport, the above relation (RHS of eq.(9)) includes by following factors: blob velocity, correlation length in the radial direction, the blobs amplitude, and the blobs passing frequency. The velocity is already discussed in the eq.(6). Remaining parameters may determine the factor $(\alpha\beta)^{-1/5}$. We investigated space-time correlation of turbulence-driven flux like FIG.2. for low α (α = 3.0 x 10^{-6}, β = 6.0 x 10^{-4}), high α (α = 4.8 x 10^{-5}, β = 6.0 x 10^{-4}), low β (α = 3.0 x 10^{-5}, β = 3.0 x 10^{-4}), and high β (α = 3.0 x 10^{-5}, β = 6.0 x 10^{-3}) cases. However, the dependence of radial correlation length on α and β is not distinctive. Thus, α and β dependency on the D_{eff} through the radial correlation length might be weak. Next, we plot the time evolutions of the poloidally averaged turbulence-driven flux at $x = L_x / 4$. The α dependency is shown in FIG.7., and the β dependency is ilustrated in FIG.8. It can be observed that the amplitude of the turbulence-driven flux is depending on α negatively, thus large α makes the D_{eff} small. This is consistent with eq.(9). Although the origin of β-dependence of the coefficient $(\alpha\beta)^{-1/5}$ in eq.(9) has not been completely identified, it is suggested that the origin of the factor $(\alpha\beta)^{-1/5}$ might be attributed to the amplitude of the flux and the frequency qualitatively.

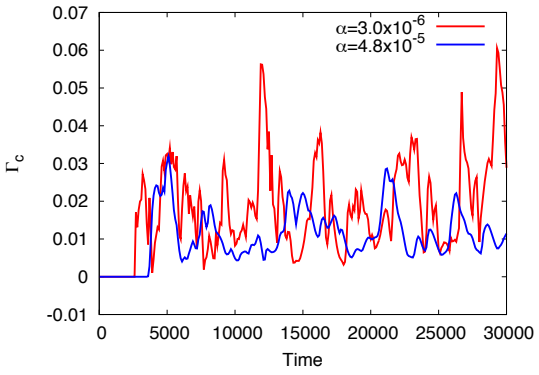

FIG. 7. Time evolution of poloidally averaged convective flux at 1/4L_x. Low α case and high α case are plotted.

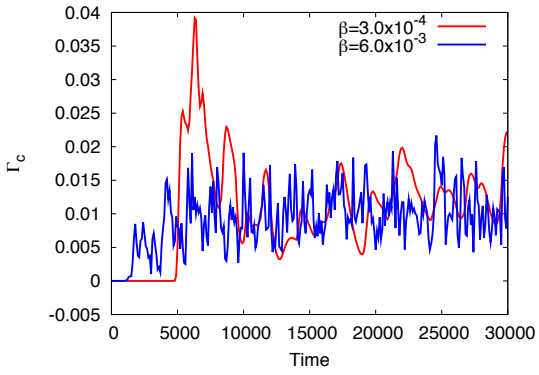

FIG. 8. Time evolution of poloidally averaged convective flux at 1/4L_x. Low β case and high β case are plotted.

4. Summary

The turbulent transport in SoL is investigated using the flux-driven nonlinear simulation that employs the 2D Hasegawa-Wakatani-type resistive interchange model. Spontaneous generation of blobs is demonstrated. During the turbulence evolution, radially-elongated meso-scale convective cells are formed autonomously and they dominate the SoL radial transport. Analyzing this phenomenon, we estimated the effective transport velocity. The effective transport coefficient is also observed and the Bohm-like dependence is also studied. To control the SoL radial transport, it might be effective to use the geometry, which take the minimum $L_{\parallel} / R$ (T / eB). It is concluded that the flux-driven turbulence induces the Bhom-like nonlocal transport. The origin of the parameter dependence of the effective transport coefficient is investigated. The transport velocity, amplitude of the turbulence, and the frequency of the turbulence might be factors.

Acknowledgements

This work is supported by Grant-in-Aid for Scientific Research (S) of Japan Scociety for Promotion of Science (JSPS) (21224014), Grant-in-Aid for Scientific Research (B) of JSPS (19360415), and Grant-in-Aid for JSPS Fellows (4534).

References

[1] LIU, H.Q., et al., "Measurement of Blob-like Structure Behavior in the Plasma Edge in QUEST", J. Plasma Fusion Res. SERIES **9** (2010) 033.
[2] THEILER, C., et al., "Study of Filament Motion and Their Active Control", 36th EPS Conference on Plasma Phys. **33E** (2009) O-5.067
[3] TANAKA, H., et al., "Statistical Analysis of Fluctuation Characteristics at High- and Low-field Sides in L-mode SOL plasmas of JT-60U", Nucl. Fusion **49** (2009) 065017,
[4] YAGI, M., et al., "Disparate Scale Nonlinear Interactions in Edge Turbulence", Contrib. Plasma Phys. **48** (2008) 13.
[5] KRASHENINNIKOV, S.I., "On Scrape off Layer Plasma Transport", Phys. Lett. A **283** (2001) 368.
[6] SUGITA, S., et al., "Nonlinear Effect on the Plasma Blob Propagation in the Scrape-off Layer", Theor. Appl. Mech. Japan **57** (2008) 207.
[7] Aydemir, A.Y., "Convective Transport in the Scrape-off Layer of Tokamaks", Phys. Plasmas **12** (2005) 06253
[8] SUGITA, S., et al., "Interchange Turbulence and Radial Transport in Tokamak Scrape-off Layer Dominated by Meso Scale Structure", J. Phys. Soc. Japan **79** (2010) 044502.
[9] KADMTSEV, B.B., "Plasma Turbulence", Academic, New York (1965).